Published in "Physica C: Superconductivity 469(14): 846-851, 2009"
which should be cited to refer to this work.

Enhanced superconducting properties of Eu_2O_3-doped MgB_2

N. Ojha [a], V.K. Malik [b], C. Bernhard [b], G.D. Varma [a,*]

[a] Department of Physics, Indian Institute of Technology Roorkee, Roorkee 247667, India
[b] Department of Physics and Fribourg Centre for Nanomaterials-FriMat, University of Fribourg, Chemin du Musee, CH-1700 Fribourg, Switzerland

Bulk polycrystalline samples of Eu_2O_3-doped MgB_2 have been synthesized by a standard solid state reaction route and their structural and superconducting properties have been investigated. As a function of Eu_2O_3 content we have found a significant increase in the critical current density (J_c) and the irreversibility field (H_{irr}) in the magnetic field range 0–6 T. The XRD results reveal the presence of MgO and EuB_6 secondary phases along with the main hexagonal phase of MgB_2. The strain values and the lattice distortions have been found to increase almost linearly with the nominal Eu_2O_3 content. The observed significant improvement in $J_c(H)$ and H_{irr} in the Eu_2O_3-doped MgB_2 samples, thus is mainly attributed to the lattice distortions introduced by Eu_2O_3 doping.

1. Introduction

The discovery of superconductivity in MgB_2 with a critical temperature, T_c around 39 K has generated great interest due to its possible technological applications [1]. Some of the important characteristics of MgB_2 which make it attractive are its simple composition, the lack of weak grain boundary connections, and the ease and low cost of production. Another important feature of MgB_2 is the presence of two superconducting gaps, which enables the tuning of H_{c2} by controlling different defect sublattices relative to the orthogonal hybrid bands. Many efforts have been made since the discovery of MgB_2 to improve its H_{c2}, H_{irr} and $J_c(H)$ to the levels required for commercial applications. These superconducting properties have been greatly improved through various synthesizing methods, such as hot isostatic pressing [2], hybrid physical–chemical vapor deposition [3] and high power ion beam ablation [4]. In addition, various dopants have been used to improve the superconducting performance of MgB_2. The substitution of C at B site by using various forms of C-containing dopants, such as SiC [5–9], C [10–13], B_4C [14,15] and some organic compounds [16–18], has been very effective in improving Hc_2. Metallic elements, such as Ca, Nb, Ti and Cu as a substitute for Mg, have also been used to improve T_c and magnetic J_c [19–21]. Introduction of fine non-superconducting particles as pinning centers is also believed to be an effective way to enhance the superconductivity [22]. Doping of magnetic impurity generally deteriorate the superconducting properties [23–25]. However, some recent work on rare earth oxides doped MgB_2 have shown improvement in $J_c(H)$ and H_{irr} [26–29]. It has been reported that doped rare earth oxides give rise to REB_6 and REB_4 impurities phases embedded into the MgB_2 matrix which lead to improvement in flux pinning.

In the present work, we have studied the effect of Eu_2O_3 doping on the structural and superconducting properties of MgB_2. We have seen a significant improvement in $J_c(H)$ and H_{irr}.

2. Experimental

The polycrystalline samples of Eu_2O_3-doped MgB_2 with nominal compositions $Mg_{1-x}(Eu_2O_3)_{x/2}B_2$ (x = 0.0, 0.01, 0.02, 0.03, 0.04 and 0.05) were synthesized by a standard solid state reaction method. Magnesium powder (Mg, purity 99%), amorphous boron (B, purity 99%) and Eu_2O_3 (purity 99%) were used as starting materials. The appropriate amounts were mixed and ground. The resulting powder was pelletized with a hydraulic press in form of rectangular pellets. The pellets were sintered at ~850 °C in Ar–H_2 (Ar:H_2 = 9:1) atmosphere for ~3 h followed by furnace cooling down to room temperature. Henceforth the samples synthesized with compositions x = 0.0, 0.01, 0.02, 0.03, 0.04 and 0.05 will be represented as MBE0, MBE1, MBE2,

* Corresponding author. Tel.: +91 1332 285353; fax: +91 1332 286662.
E-mail address: gdvarfph@iitr.ernet.in (G.D. Varma).

MBE3, MBE4 and MBE5, respectively. The phase identification of the samples was carried out using X-ray diffractometry with Cu–Kα radiation. The microstructure of the samples was studied using a field emission scanning electron microscope (FESEM). Magnetization measurements of the samples were done using a Physical Properties Measurement System (PPMS Quantum Design-6000). Magnetic J_c values were calculated from the magnetization loops by using Bean model.

3. Results and discussion

Fig. 1 shows the X-ray diffraction (XRD) patterns of the samples synthesized with nominal compositions $Mg_{1-x}(Eu_2O_3)_{x/2}B_2$ (x = 0.0, 0.01, 0.02, 0.03, 0.04 and 0.05). The XRD pattern of sample MBE0 reveals the presence of the hexagonal phase of MgB_2 with traces of MgO impurities. The XRD patterns of the Eu_2O_3-doped samples show, besides the main MgB_2 phase, the presence of MgO and EuB_6 secondary phases. No traces of unreacted Eu_2O_3 or any other oxides of Eu have been found through XRD results. It has been found that the peak intensities of EuB_6 peaks increase with increase in Eu_2O_3 content, whereas the peak intensity of MgO remains almost constant. We have estimated the strain value and crystallite size of the samples from the Williamson–Hall plot. We find that the average crystallite size of the sample MBE1 has a smaller value as compared to the sample MBE0. The crystallite size, however, increases with further increase in concentration of Eu_2O_3. The strain in the sample increases almost linearly with concentration of Eu_2O_3 (see Fig. 2) and [Table 1]. The linear increase in strain values with x is suggestive of a corresponding increase in lattice defect in the doped samples. We have synthesized the samples with nominal compositions $Mg_{1-x}(Eu_2O_3)_{x/2}B_2$ (x = 0.0, 0.01, 0.02, 0.03, 0.04 and 0.05), i.e. we are decreasing the content of Mg with

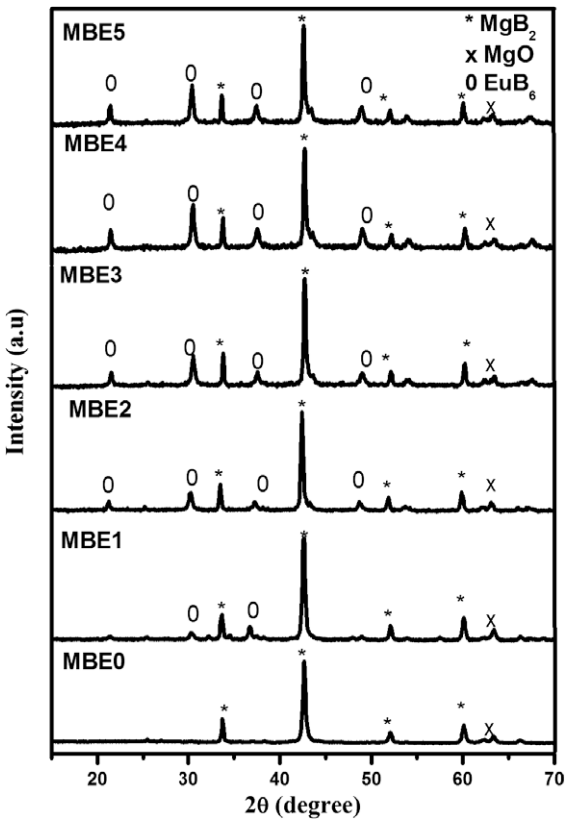

Fig. 1. XRD patterns of Eu_2O_3-doped MgB_2 synthesized with nominal compositions $Mg_{1-x}(Eu_2O_3)_{x/2}B_2$ (x = 0.0, 0.01, 0.02, 0.03, 0.04 and 0.05).

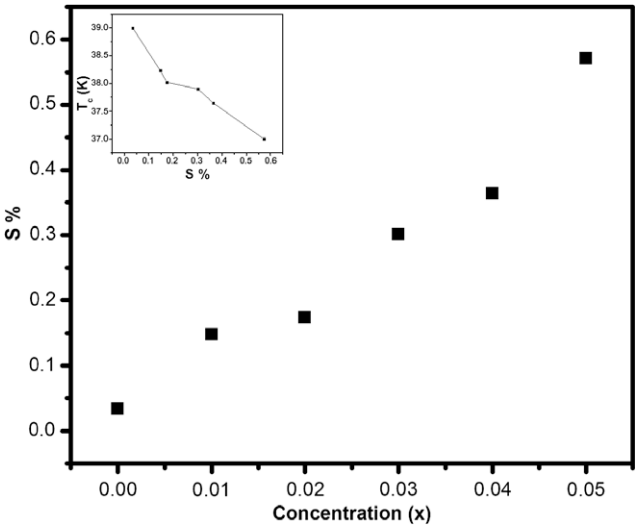

Fig. 2. Variation of lattice strain (S%) with concentration (x). Inset shows variation of T_c with lattice strain (S%).

increase in the Eu_2O_3 concentration. Therefore there is chance of Mg vacancies and presence of oxygen in the lattice of doped samples. These lead to lattice defects and hence to an increase in the strain values. Earlier Serquis et al. [30] also observed that strain linearly increases with decrease in Mg occupancy in MgB_2 samples. From the XRD results we find that lattice parameters a and c increase when value of x increases from 0.0 to 0.01. The lattice parameters, however, start decreasing with further increase in x values (see Table 1). The initial increase in the lattice parameters may be due to partial substitution of Eu at Mg site of MgB_2 [28]. For x > 0.01, the decrease in the lattice parameters with increasing Eu_2O_3 content (x) in the samples may be due to increased values of strain.

Fig. 3 shows the FESEM micrographs of the Eu_2O_3-doped and the pure MgB_2 samples. The micrographs of samples MBE0 and MBE1 show the presence of fine grains. The grain size increases when the Eu_2O_3 content in the sample exceeds x = 0.01. These results are in conformity with the XRD results. From the FESEM micrographs it is also clear that the homogeneity of the microstructure is greatest for the undoped sample and it decreases with increasing Eu_2O_3 content. However, the connectivity of the grains is better in the samples with higher Eu_2O_3 concentration. This shows that the secondary EuB_6 phase precipitates at the boundaries of the MgB_2 grains.

The resistance vs temperature (R–T) and magnetization vs temperature (M–T) measurements (figures not shown here) show that the T_c values of the samples decreases from 39 to 37 K, when x increases from x = 0 to 0.05. The decrease in T_c may be related to the increase in the lattice distortions (Mg vacancies). We have found almost linear decrease in T_c with strain (S%) (see inset of Fig. 2). A similar decrease in T_c with increase in strain in MgB_2 has also been reported by Serquis et al. [30] and Liao et al. [31]. In addition to strain, the partial substitution of Eu at Mg site may be responsible for small reduction in T_c [28]. We have also seen a decrease in the residual resistivity ratio (RRR = R_{295K}/R_{40K}) values with increase in x (see Table 1). The decrease in RRR values with x again confirms the presence of lattice defects/distortions in the doped samples which enhance the impurity scattering.

The magnetic J_c of all the samples at 10 and 20 K have been calculated from the M–H loops using the Bean model [32]. The average grain sizes required in the Bean formula have been determined from the FESEM micrograph (see Table 1). The M–H loops of MBE0,

Table 1
Values of J_c, lattice parameters, strain, RRR, A_F and H_{irr} (T) of Eu_2O_3-doped MgB_2.

Samples	J_c (A/cm^2)		Lattice parameter (Å)		Strain (%)	RRR (R_{295}/R_{40})	A_F	H_{irr} (T) 10 K	Grain size (μm)
	10 K, 2 T	20 K, 2 T	*a*	*c*					
MBE0	1.34×10^3	1.30×10^2	3.0767	3.5186	0.03391	3.35	0.14	2.75	0.651
MBE1	2.54×10^4	8.66×10^2	3.0981	3.5275	0.14732	3.67	0.18	5.99	0.569
MBE3	2.88×10^4	1.88×10^3	3.0780	3.5176	0.30137	3.12	0.21	4.47	0.429
MBE4	6.05×10^4	4.86×10^3	3.0574	3.5116	0.36335	2.96	0.25	4.46	0.441
MBE5	7.68×10^4	7.71×10^3	3.0583	3.5171	0.57083	2.56	0.26	5.55	0.560

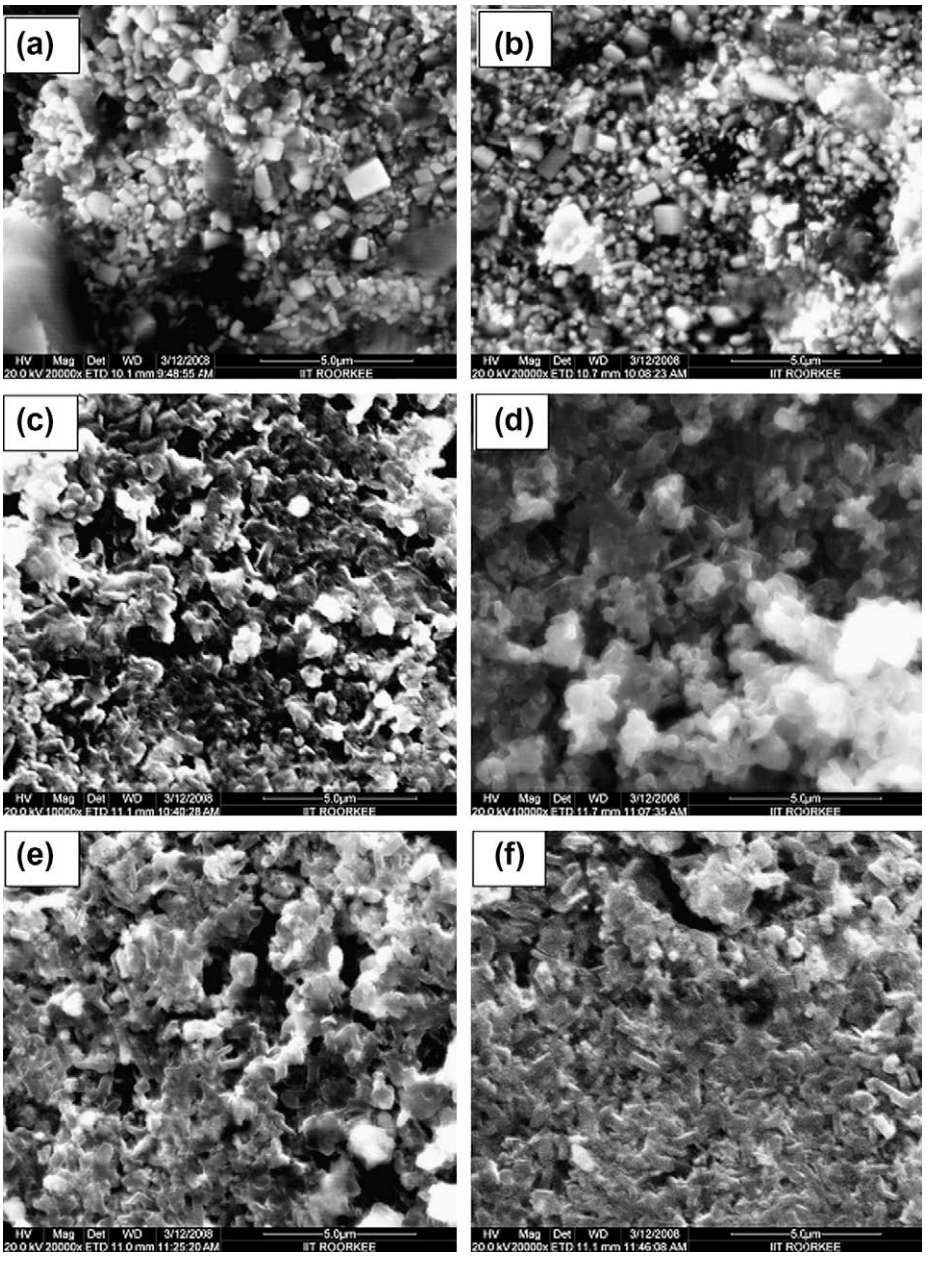

Fig. 3. FESEM micrographs: (a) MBE0, (b) MBE1, (c) MBE2, (d) MBE3, (e) MBE4, and (f) MBE5.

MBE1, MBE3, MBE4 and MBE5 measured at 10 and 20 K are shown in Fig. 4. The field dependence of J_c measured at 10 and 20 K is shown in Fig. 5. From this figure it is clear that in the field range 0–4 T the J_c values increases with increase in Eu_2O_3 content (x) at both temperatures. At higher field (>5.5 T) the J_c values of sample MBE3 are higher than for the other samples (see Fig. 5). It is also seen that the J_c values of the doped samples decrease more slowly with field as compared to the undoped sample. This means there is better flux pinning in the doped samples. The J_c values of the samples MBE0, MBE1, MBE3, MBE4 and MBE5 at 2 T field and measured at 10 and 20 K are given in Table 1. We can see that at 2 T and 10 K the J_c value increases from 1.34×10^3 A/cm^2 to

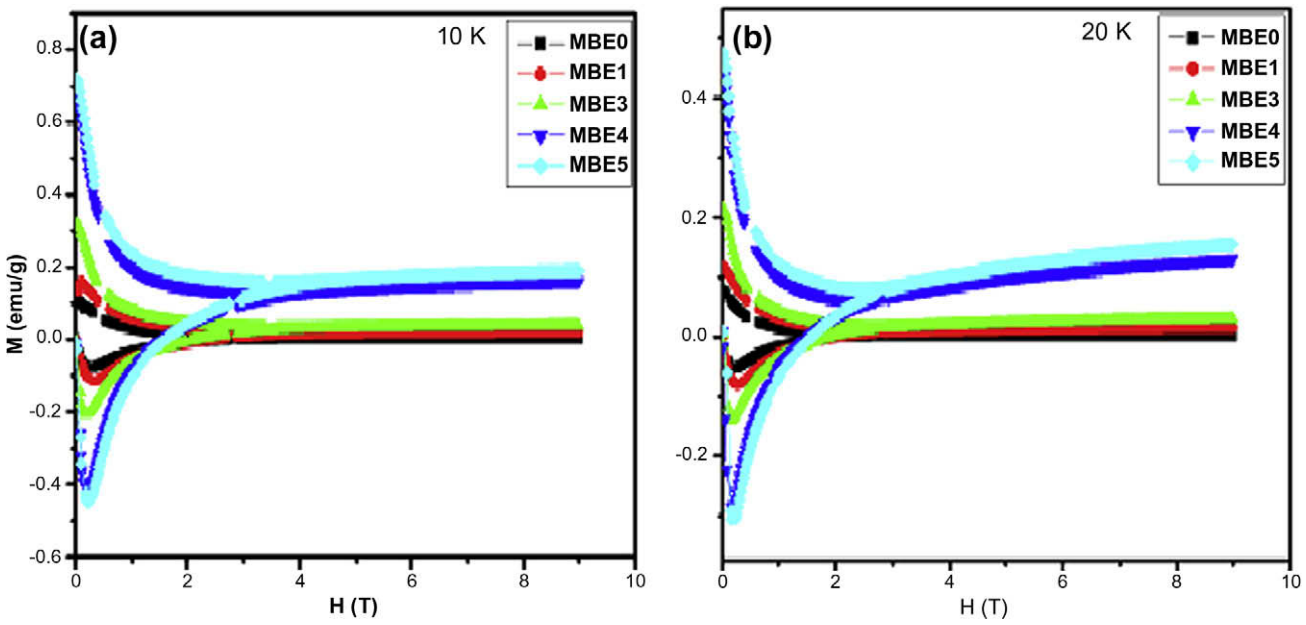

Fig. 4. M–H loops of Eu_2O_3-doped MgB_2 measured at 10 K (a) and at 20 K (b).

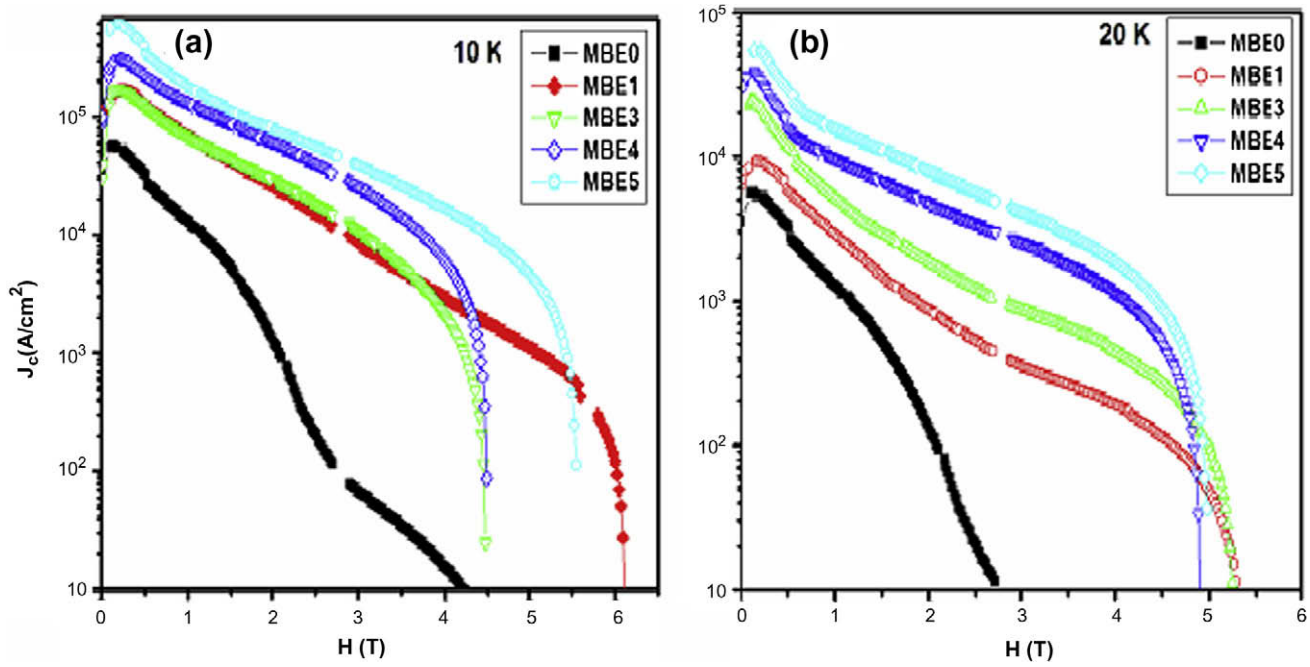

Fig. 5. Field dependence of J_c of Eu_2O_3-doped MgB_2 (a) at 10 K and (b) at 20 K.

7.68×10^4 A/cm^2 and at 20 K it increases from 1.30×10^2 A/cm^2 to 7.71×10^3 A/cm^3 when x increases from 0 to 0.05. Thus there is a more than about 500-fold enhancement in the J_c value of sample MBE5 at 2 T field with respect to undoped sample. Another noticeable point from the M–H loops is that the M–H loops of the doped samples shift up and down from the magnetic axis as magnetic field increases (see Fig. 4). This means there is paramagnetic phase present along with the superconducting phase [29]. Since neither MgB_2 nor MgO are paramagnetic, the EuB_6 impurity phase (detected through XRD) is suspected to be paramagnetic. Thus, the magnetic secondary phase present in the doped samples is expected to act as stronger flux pinning centers leading to enhancement in $J_c(H)$ of the doped samples [29]. In addition to this, the defects centers in the doped samples act as flux pinning centers leading to improvement in $J_c(H)$.

The connection factor A_F was also evaluated by the resistivity phonon term according to Rowell analysis [33]. It has been observed that A_F increases with increase in the concentration of Eu_2O_3 in the sample. The increase in A_F in Eu_2O_3-doped MgB_2 signals a better connectivity between the grains which is consistent with the FESEM micrographs (Fig. 3). Thus better connectivity between the grains and improvement in flux pinning force are expected to be responsible for the improvement in $J_c(H)$ of the doped samples.

To confirm that the improvement in $J_c(H)$ of the Eu_2O_3-doped MgB_2 is due to an improved flux-pinning behavior, we have calculated the flux pinning force (F_p) from the M–H curves, recorded at 10 K and 20 K, by using the relation [34,35]

$$F_p = J_c(H) \times H(T) \quad (1)$$

The variation of $F_p/F_{p,max}$ with field is shown in Fig. 6. This figure is consistent with the $J_c(H)$–H plots (Fig. 5). From the figure it is clear that the pinning force curves of the doped samples shift toward the high field side indicating an improvement in flux pinning for the doped samples. The better flux pinning in the doped samples is possibly due to presence of defect centers and paramagnetic impurity phase EuB_6.

The values of the irreversibility field $H_{irr}(x)$ have been estimated from the M–H loops measured at 10 and 20 K. In the present work H_{irr} is taken as the field at which J_c becomes ~100 A/cm^2. The values of H_{irr} are given in Table 1. Fig. 7a shows the variation of H_{irr} with doping level x. It shows that the H_{irr} value first increases from $x = 0$ to $x = 0.01$ but it decreases with further increase in x. However, the H_{irr} values of doped samples are higher as compared to the undoped samples. We have also plotted the variation of the full width half maximum (FWHM) of the (1 0 1) peak of XRD pattern with x (Fig. 7b). The comparison of Fig. 7a and b reveals that the FWHM of the (1 0 1) peak and H_{irr} both vary in a similar manner with doping level up to $x = 0.04$, i.e. when H_{irr} is high, the XRD peak of the corresponding sample is broadened, and vice versa. Similar correlation between H_{irr} and FWHM has been reported by Yamamoto et al. [36] who observed that the FWHM of the (1 0 0) peak, which also corresponds to distortion of the honeycomb boron sheet in MgB_2, has a positive correlation with the H_{irr} of MgB_2, that is H_{irr} increases with increasing FWHM of (1 0 0) peak. In the present case we have seen an increase in strain values in the doped samples because of lattice distortions in the samples. The lattice distortions lead to enhancement in the H_{irr} values of the doped samples.

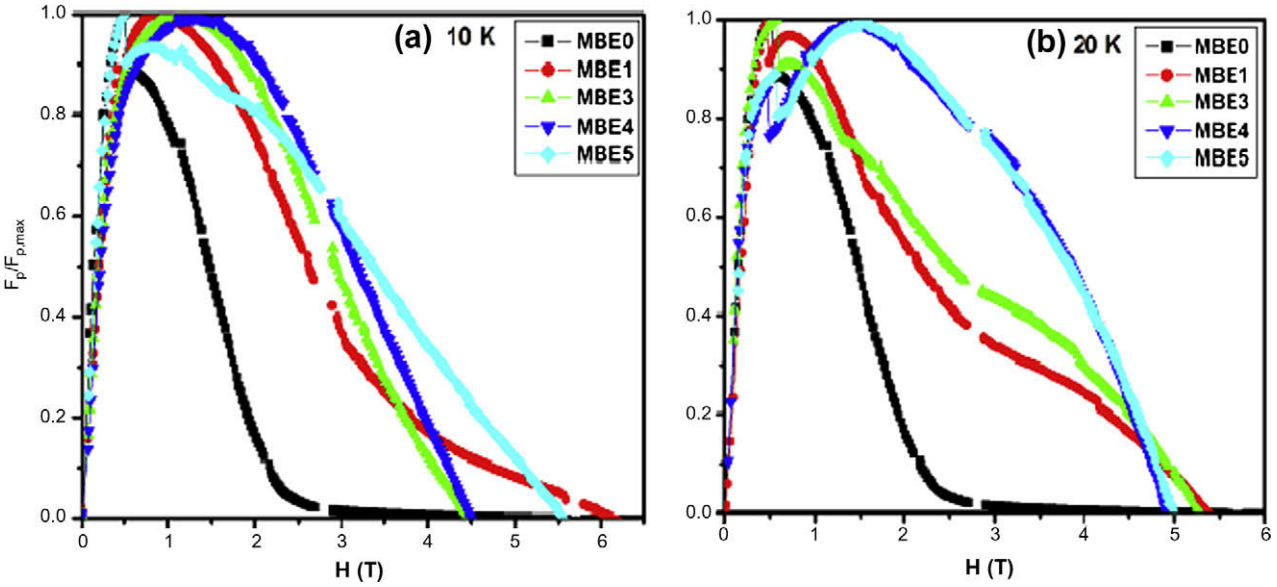

Fig. 6. $F_p/F_{p,max}$ versus magnetic field plots of Eu_2O_3-doped MgB_2 (a) at 10 K and (b) at 20 K.

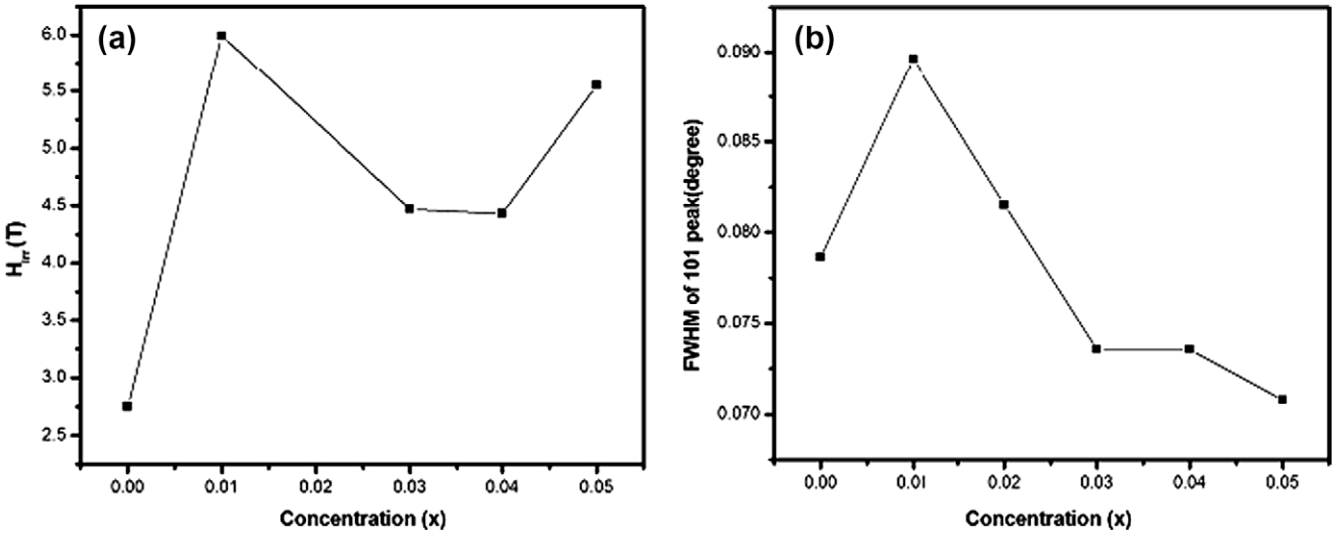

Fig. 7. Variation of H_{irr} (T) (at 10 K) and FWHM with doping concentration (x).

4. Conclusions

In the present work we have seen significant improvement in H_{irr} and $J_c(H)$ of Eu_2O_3-doped MgB_2. It is thought that defects and paramagnetic impurity phase EuB_6 in the doped samples provide better flux pinning leading to improvement in $J_c(H)$.

Acknowledgements

This work was supported by M.H.R.D (Govt. of India), C.S.I.R. (Govt. of India) and by the Schweizer National fonds (SNF) by Grant 200020–119784. We are thankful to Dr. R. Rawat (UGC-DAE CSR, Indore Centre) for doing R–T measurements in magnetic field.

References

[1] J. Nagamatsu, N. Nakagawa, T. Muranaka, Y. Zenitani, J. Akimitsu, Nature 410 (2001) 63.
[2] A. Serquis, L. Civale, D.L. Hammon, X.Z. Liao, J.Y. Coulter, Y.T. Zhu, M. Jaime, D.E. Peterson, F.M. Muller, V.F. Nesterenko, Y. Gu, Appl. Phys. Lett. 82 (2003) 2847.
[3] M. Iavarone, G. Karapetrov, A. Menzel, V. Komanicky, H. You, W.K. Kwok, P. Orgiani, V. Ferrando, X.X. Xi, Appl. Phys. Lett. 87 (2005) 242506.
[4] Y. Fudamoto, T.J. Renk, G.A. Torres, N. Kishimoto, Phys. Rev. B 250 (2006) 320.
[5] S.X. Dou, S. Soltanian, J. Horvat, X.L. Wang, S.H. Zhou, M. Ionescu, H.K. Liu, P. Munroe, M. Tomsic, Appl. Phys. Lett. 81 (2002) 3419.
[6] H. Kumakura, H. Kitaguchi, A. Matsumoto, H. Hatakeyama, IEEE Trans. Appl. Supercond. 15 (2005) 3184.
[7] S. Soltanian, X.L. Wang, J. Horvat, S.X. Dou, M.D. Sumption, M. Bhatia, E. Collings, P. Munroe, M. Tomsic, Supercond. Sci. Technol. 18 (2005) 658.
[8] A. Yamamoto, J. Shimoyama, S. Ueda, Y. Katsura, S. Horii, K. Kishio, IEEE Trans. Appl. Supercond. 15 (2005) 3292.
[9] S.C. Yan, G. Yan, Y.F. Lu, L. Zhou, Supercond. Sci. Technol. 20 (2007) 549.
[10] Y.W. Ma, X.P. Zhang, J. Nishijima, K. Watanabe, S. Awaji, X.D. Bai, Appl. Phys. Lett. 88 (2006) 072502.
[11] R.H.T. Wilke, S.L. Bud'ko, P.C. Canfield, D.K. Finnemore, R.J. Suplinskas, S.T. Hannahs, Phys. Rev. Lett. 92 (2004) 217003.
[12] W.K. Yeoh, J.H. Kim, J. Horvat, X. Xu, S.X. Dou, Physica C 460 (2007) 568.
[13] S.C. Yan, G. Yan, L. Zhou, Y. Jia, H.H. Wen, Y.F. Lu, Supercond. Sci. Technol. 20 (2007) 377.
[14] W. Mickelson, J. Cumings, W.Q. Han, A. Zettl, Phys. Rev. B 65 (2002) 052505.
[15] A. Yamamoto, J. Shimoyama, S. Ueda, I. Iwayama, S. Horii, K. Kishio, Supercond. Sci. Technol. 18 (2005) 1323.
[16] J.H. Kim, S. Zhou, M.S.A. Hossain, A.V. Pan, S.X. Dou, Appl. Phys. Lett. 89 (2006) 142505.
[17] B.H. Jun, C.J. Kim, Supercond. Sci. Technol. 20 (2007) 980.
[18] J.H. Kim, X. Xu, M.S.A. Hossain, D.Q. Shi, Y. Zhao, X.L. Wang, S.X. Dou, S. Choi, T. Kiyoshi Appl. Phys. Lett. 92 (2008) 042506.
[19] T. Prikhna, W. Gawalek, Y. Savchuk, N. Sergienko, V. Moshchil, S. Dub, V. Sverdun, L. Kovalev, V. Penkin, M. Zeisberger, M. Wendt, G. Fuchs, T. Habisreuther, D. Litzkendorf, P. Nagorny, V. Melnikov, Physica C 460 (2007) 595.
[20] Y.X. Sun, D.L. Yu, Z.Y. Liu, T.S. Wang, J.L. He, J.Y. Xiang, D.N. Zheng, Y.J. Tian, Supercond. Sci. Technol. 20 (2007) 261.
[21] H.X. Geng, G.C. Che, W.W. Huang, S.L. Jia, H. Chen, Z.X. Zhao, Supercond. Sci. Technol. 20 (2007) 452.
[22] A. Yamamoto, J. Shimoyama, S. Ueda, S. Horii, K. Kishio, Physica C 445 (2006) 801.
[23] M. Kuhberger, G. Gritzner, Physica C 370 (2002) 39.
[24] H. Kitaguchi, H. Kumakura, Supercond. Sci. Technol. 18 (2005) S284.
[25] C.H. Cheng, Y. Zhao, X.T. Zhu, J. Nowotny, C.C. Sorrell, T. Finlayson, H. Zhang, Physica C 386 (2003) 588.
[26] J. Wang, Y. Bugoslavsky, A. Berenov, L. Cowey, A.D. Caplin, L.F. Cohen, L.D. Cooley, X. Song, D.C. Labalestier, Appl. Phy. Lett. 81 (2005) S284.
[27] S.K. Chen, M. Wei, J.L. Mscmanus-Driscoll, Appl. Phys. Lett. 88 (2006) 192512.
[28] T. Katsura, J. Shimoyama, A. Yamamoto, S. Horii, K. Kishio, Physica C 461 (2007) 225.
[29] C. Cheng, Y. Zhao, Appl. Phys. Lett. 89 (2006) 252501.
[30] A. Serquis, Y.T. Zhu, E.J. Peterson, J.Y. Coulter, D.E. Peterson, F.M. Mueller, Appl. Phys. Lett. 79 (2001) 4399.
[31] X.Z. Liao, A. Serquis, Y.T. Zhu, D.E. Peterson, F.M. Mueller, H.F. Xu, Supercond. Sci. Technol. 17 (2004) 1026.
[32] C.P. Beans, Rev. Mod. Phys. 36 (1964) 31.
[33] J.M. Rowell, Supercond. Sci. Technol. 16 (2003) R17.
[34] E. Martinez, P. Mikheenko, M. Martinez-lopez, A. Millan, A. Bevan, J.S. Abell, Phys. Rev. B 75 (2007) 134515.
[35] T.M. Shen, G. Li, C.H. Cheng, Y. Zhao, Supercond. Sci. Technol. 19 (2006) 1219.
[36] A. Yamamoto, J. Shimoyama, S. Ueda, Y. Katsura, I. Iwayama, S. Horii, K. Kishio, Appl Phys. Lett. 86 (2005) 212502.